Hierarchical Coordination of a Community Microgrid With AC and DC Microgrids

Liang Che, *Student Member, IEEE*, Mohammad Shahidehpour, *Fellow, IEEE*, Ahmed Alabdulwahab, and Yusuf Al-Turki

***Abstract*—In this paper, a community microgrid with multiple ac and dc microgrids is introduced and analyzed. Individual microgrids with different frequency and voltage requirements would operate as self-controlled entities, which could also cooperate with neighboring microgrids for providing back-up operations in the community microgrid. A hierarchical coordination strategy with primary, secondary, and tertiary coordination is proposed for the economic operation of an islanded community microgrid. The hierarchical strategy is also applied to a grid-connected community microgrid and the results are discussed. The simulation results verify that the proposed hierarchical coordination strategy is an effective and efficient way for coordinating microgrid flows in an islanded community microgrid, while maintaining the rated frequency and voltage with each microgrid. The simulation results also demonstrate the economic operation of a grid-connected community microgrid in which individual microgrids operate as autonomous agents, while satisfying the community objectives.**

***Index Terms*—AC and dc microgrids, community microgrid, droop function, economics and reliability, hierarchical control, hybrid microgrid, microgrid islanding.**

NOMENCLATURE

Variables

e_j, e_j^{2nd}	Per-unit error signals in the primary and secondary coordination at microgrid $(\text{MG})_j$.
$f_0, f_j, V_{\text{DC},j}$	Frequency and dc voltage in MG_0 and in ac or dc MG_j.
m_P, m_Q, R	Microgrid droop control parameters.
m_j	Coordination parameter at converter interlinking-converter $(\text{IC})_j$.
$P^{\text{ref}}, Q^{\text{ref}}, I^{\text{ref}}$	Reference values of power and current for droop control within microgrids.
$P_{\text{gen},j}, P_{\text{load},j}$	Total generation and load in MG_j.
$P_{X,j}, P_{X,j}^{\text{ref}}$	Power exchange and its reference value of MG_j (positive values for exported power).

Parameters

$f_j^{\text{rated}}, V_{\text{DC},j}^{\text{rated}}$	Rated values of frequency and dc voltage in ac or dc MG_j.
N	Number of the converter-coupled microgrids (MG_j) in a community microgrid.

Indices

j, k	Indices of a converter-coupled microgrid in a community microgrid ($j, k = 1, 2, \ldots, N; j \neq k$).

Manuscript received July 5, 2014; revised November 5, 2014 and January 8, 2015; accepted January 25, 2015. This work was supported by the National Science, Technology, and Innovation Plan Strategic Technologies Program in the Kingdom of Saudi Arabia under Project 13-ENE2411-03. Paper no. TSG-00688-2014.

L. Che is with the Galvin Center for Electricity Innovation, Illinois Institute of Technology, Chicago, IL 60616 USA.

M. Shahidehpour is with the Galvin Center for Electricity Innovation, Illinois Institute of Technology, Chicago, IL 60616 USA, and also with the Renewable Energy Research Group, King Abdulaziz University, Jeddah 21589, Saudi Arabia (e-mail: ms@iit.edu).

A. Alabdulwahab and Y. Al-Turki are with the Department of Electrical and Computer Engineering, Renewable Energy Research Group, King Abdulaziz University, Jeddah 21589, Saudi Arabia.

Color versions of one or more of the figures in this paper are available online at http://ieeexplore.ieee.org.

Digital Object Identifier 10.1109/TSG.2015.2398853

I. INTRODUCTION

MICROGRIDS are introduced into electric power systems for managing the widespread penetration of renewable energy and distributed generations (DGs) in power distribution networks [1]–[2]. AC microgrids, which are connected to the utility grid at the point of common coupling (PCC), represent the most studied microgrid structure [3]–[6]. DC microgrids have attracted additional attentions in recent years due to the proliferation of solar photovoltaic (PV) and energy storages and the growth of dc loads such as data centers and LED lighting [7].

Droop-based hierarchical strategy which includes primary, secondary, and tertiary control is introduced to facilitate flexible and efficient operations of ac microgrids [8]–[10] and dc microgrids [11], [12]. In addition to providing a straightforward interface to dc loads, dc microgrids would offer simpler control strategies and resynchronization processes, and enhance power quality as there are no variations in frequency or reactive power.

Due to the increasing of dc sources and loads in the ac-dominated world, interests on hybrid ac/dc microgrids are growing rapidly. In general, a hybrid microgrid is defined as a microgrid combining both ac and dc systems where only the ac sub-grid connects to the main grid, with the associated advantages of reducing the processes of power conversions and facilitating the integration of ac and dc sources and loads to power system [13]. Extensive research efforts have been put into the coordination control of hybrid microgrid [13]–[17], where the bidirectional interlinking-converter that interfaces the dc sub-grid to the ac sub-grid plays a critical role in the operation of a hybrid microgrid.

A multimicrogrid or community microgrid is formed when a cluster of neighboring microgrids is linked via interlinking-converters. In a community microgrid, individual microgrids may possess their own specific frequency and voltage requirements and operate as self-controlled and autonomous entities. Individual microgrids might also cooperate with neighboring microgrids for providing back-up operations in emergencies and for economic purposes. Community microgrid would merge the advantages of ac and dc microgrids and additionally improve the reliability and economic performance of individual microgrid systems. Individual microgrids would have their respective connections to the main grid while also interconnected with other microgrids in the community.

The community microgrid is different from a hybrid microgrid as the latter is mostly a single microgrid which blends ac and dc configurations to ease the integration of dc sources and loads, while a community microgrid would coordinate a cluster of interlinking ac and dc microgrids located in adjacent areas. The interest in such microgrids is growing rapidly which is due to the increasing number of dc sources and loads in the ac-dominated arena.

Extensive research has been devoted to the coordinated control strategy of hybrid microgrids [13]–[17], where the bidirectional interlinking-converter, that interfaces the ac and dc sub-grids, plays a critical role in the hybrid microgrid operation. Reference [18] provides a preliminary review of the community microgrid concept, in which "microgrid-like regions" connected by "controllable interconnection ties" directly communicate with their adjacent regions. References [19] and [20] present the architecture and advantages of a community microgrid in which each microgrid is connected to the main grid while also interconnected by a common dc bus to other microgrids in the community. However, previous papers did not provide a detailed formulation for the implementation and the coordinated control of a community microgrid.

The implementation of a community microgrid requires an efficient strategy to coordinate the power exchange among participating microgrids, especially when operating the community as an island. The coordination strategy proposed in this paper is initially inspired by studies cited in [13] and [14]. In [14], a coordination control approach of a hybrid microgrid is proposed. This approach would initiate the power exchange between ac and dc sub-grids in a decentralized manner based on a coordination droop designed at the interlinking-converter; but such power exchange would be determined by interlinking-converter droop coefficients and may cause frequency or voltage deviations in steady state. In this paper, we extend the application of such interlinking-converter droop to the coordination of multiple ac and/or dc microgrids in a community microgrid, and propose a novel three-level hierarchical coordination strategy to regulate the islanded and grid-connected optimal power exchanges among neighboring microgrids.

Major contributions of this paper are listed as follows.

1) The interlinking-converter droop is modified and applied to the coordination of a community microgrid.
2) A hierarchical coordination strategy is proposed for the flexible and the optimal coordination of power exchanges while maintaining the normal operation of participating microgrids.

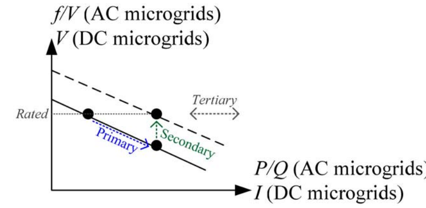

Fig. 1. Droop control in ac and dc microgrids.

3) A standardized community microgrid architecture, as well as its operational features, are presented.

The novelty of the proposed coordination strategy will be further highlighted in Section V by comparing the proposed strategy with the existing microgrid droop control methodologies.

II. Droop Control in AC and DC Microgrids

AC and dc microgrids adopt a droop-based hierarchical control strategy in grid-connected and island modes [9]–[11]. This hierarchical strategy, as adopted at Illinois Institute of Technology (IIT) microgrid, includes primary, secondary, and tertiary control [6], [10]. Distributed energy resources (DERs) in a microgrid are categorized into grid-forming and grid-following operations. The grid-forming DERs (e.g., gas-turbine units, energy storages) which are capable of regulating the frequency and/or voltage (f/V) and behaving as slack bus in islanded microgrids, would implement the hierarchical droop control of microgrids.

A. Primary and Secondary Control of AC/DC Microgrids

The ac and dc microgrid droops are shown in Fig. 1, in which ac microgrids have the real power (f-P) and reactive power (V-Q) droops while dc microgrids utilize voltage versus current (V-I) droop. The droop characteristics of ac and dc microgrids are represented by (1) and (2), respectively, where m_P, m_Q, and R are the droop coefficients that determine the sensitivity of primary control

$$\begin{cases} f^{\text{rated}} - f = m_P \cdot \left(P - P^{\text{ref}}\right) \\ V^{\text{rated}} - V = m_Q \cdot \left(Q - Q^{\text{ref}}\right) \end{cases} \tag{1}$$

$$V^{\text{rated}} - V = R \cdot \left(I - I^{\text{ref}}\right). \tag{2}$$

The primary droop control applies load sharing in real-time without any communications among parallel DERs. In grid-connected mode, the f/V characteristic of microgrids is maintained by the utility grid, while in the island mode, it is maintained by the secondary control. As illustrated in Fig. 1, the secondary control would restore the rated f/V by vertically shifting the droop curve.

In order to maintain the rated power/current characteristic of DERs, the droop coefficients are adjusted by extending the droop curve shown by the solid curve in Fig. 2. In this figure, the dashed curve represents the DERs terminal frequency after enabling the secondary control function. The power output at point-B (P_B) corresponds to a threshold value above which (i.e., in the shaded zone) the frequency would start to drop even with secondary control. This is because the frequency adjustment by secondary control is limited by the DER

This article has been accepted for inclusion in a future issue of this journal. Content is final as presented, with the exception of pagination.

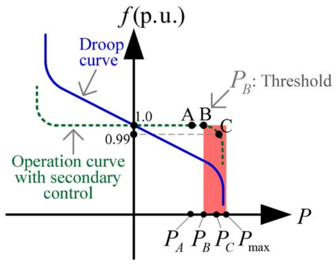

Fig. 2. Power flow limit of primary and secondary droop controls.

power output. This frequency drop indicates that the microgrid may need to import power if the load continues to increase or if portions of available generation are on outage. The f-P analyses in Fig. 2 would equally correspond to the V-Q droop in ac microgrids and V-I droop in dc microgrids.

B. Tertiary Control of AC/DC Microgrids

The economic and optimal operation of microgrids necessitates an upper level tertiary control. The master controller (MC) is the critical component in tertiary control, while building controllers, meters, phasor measurement units, and the supervisory control and data acquisition would also facilitate the implementation of tertiary control. The MC determines the hourly optimal solution at base case (steady state) condition and contingencies and sends control signals to on-site generations, storage, switches, and building controllers. The MC can also charge or discharge energy storages and control power exchanges between microgrids and utility grid for cost-efficient operations of microgrids in the grid-connected mode.

III. Structure of Community Microgrid

The community microgrid structure would enhance the reliability and the economics of the community power supply, as community loads are supplied by individual microgrids based on their rated f/V and individual microgrids would also supply backup generation for other microgrids in the community. Optimal power exchange would allow individual microgrids to reduce their installed capacity requirement which could be a critically beneficial issue in congested metropolitan communities.

Fig. 3 shows the schematic of our proposed community microgrid, based on which the proposed hierarchical coordination strategy is realized.

1) MC_0 is a directly-connected ac microgrid. MG_j ($j = 1, \ldots, N$) are ac or dc microgrids coupled by their interlinking-converters ($\text{IC}_j,\ j = 1, \ldots, N$).
2) Individual microgrids have their respective connections to the utility grid. In the community, individual microgrids are linked together by an ac main bus and could exchange power and provide backup to each other via the ac main bus.
3) Each individual microgrid is equipped with a MC (MC_0 or $\text{MC}_j, j = 1, \ldots, N$) which communicates with the central MC (CMC) through low-bandwidth communication channels. CMC supervises the entire community microgrid.

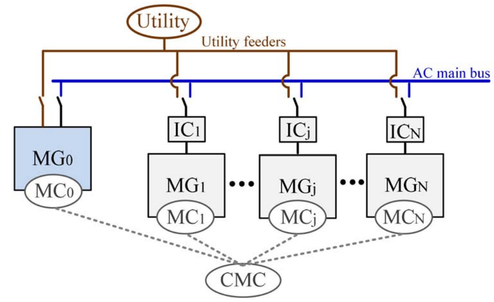

Fig. 3. Proposed standardized community microgrid architecture.

4) ICs essentially provide buffers between microgrids so that each microgrid can operate at its own rated f/V. IC_j is an ac–dc converter when MG_j is a dc microgrid; while if MG_j is an ac microgrid then IC_j would be ac–ac or ac–dc–ac type to handle the f/V variations.

The merits of the proposed structure shown in Fig. 3 are listed as follows.

1) Communication channel is eliminated between any two microgrids. The proposed hierarchical coordination strategy is implemented at each IC_j and optimized by CMC, based on which the power exchange among microgrids is initiated in a decentralized and autonomous manner. Thus no need for individual microgrids to communicate with each other to require such exchange. The proposed hierarchical coordination strategy will be discussed in Section V.
2) No high-bandwidth communication channel is required between CMC and each MC. An efficient centralized management function is considered in which CMC communicates the operating set-points to each MC through low-bandwidth channels at relatively large time intervals.
3) Here the elimination of communication channels described in 1) and 2) above is highly desirable. Because either high-bandwidth channels or communication between any two microgrids is uneconomical and unpractical due to the associated complexity, much higher cost, risk of communication failure, and low robustness derived from communication parameter uncertainties.
4) The presence of MG_0 in Fig. 3 would greatly facilitate the implementation of proposed coordination strategy. Acting as a slack bus in the islanded community system, MG_0 would efficiently respond to power exchange initiated by any MG_j. This subject will be discussed in Section V-A.
5) The proposed structure in Fig. 3 also greatly improves the reliability performance of each microgrid, since the presence of ac main bus and MG_0 could provide each MG_j a backup access to the utility grid, in case of an unintentional islanding occurring to MG_j (e.g., due to external fault or PCC failure).

IV. Operational Features of Community Microgrid

In the community microgrid, each microgrid can operate in either grid-connected or island mode, and seamlessly transfer

This article has been accepted for inclusion in a future issue of this journal. Content is final as presented, with the exception of pagination.

TABLE I
OPERATIONAL FEATURES OF COMMUNITY MICROGRID

		MG_j is grid-connected	MG_j is islanded
Operation at the community level	CMC	Optimal regulation of power exchange by communicating with each MC_j	
	MC_j	MC_j regulates the exchange between MG_j and utility grid	Scheduling DER outputs in MG_j
	IC_j	Operating in f/V regulating mode to maintain the f/V of MG_j	[1]Hierachical Coordination of power exchange between MG_j and other microgrids
Operation within MG_j		f/V is maintained by utility grid (directly or via IC_j) while secondary droop control is disabled	f/V is controlled by grid-forming DERs with enabled secondary droop control

[1] Hierarchical Coordination strategy is discussed in Section V.

between the two modes. The proposed operation principle of a community microgrid in each mode is summarized in Table I.

A. Operation in Grid-Connected Mode

As summarized in Table I, MC_j would regulate the power exchange between MG_j and utility grid by providing set-points to its dispatchable DERs for minimizing the operation cost. IC_j would act as the slack bus for MG_j to maintain its f/V since the secondary droop control in MG_j is disabled. In addition, MG_j could exchange power with other microgrids according to the set-points from CMC by connecting to the ac main bus. For example, MG_j with peak PV output at daytime could transfer the surplus energy to its neighbors for economical purpose. The grid-connected operation of community microgrid will be simulated in Case 1 in Section VI.

B. Operation in Island Mode

In case of a utility fault, microgrids may improve their load point reliability performance by switching to island mode. The islanding can be initiated by protection devices at PCC or by MC command signals. At the instance of islanding, MCs may curtail local loads to match with local generation. Depending on the available DER capacity, portions of the curtailed load may be restored in the island mode after the microgrid operation is stabilized [9]–[11]. As stated in Table I, each microgrid in island mode will operate as a self-controlled entity. Based on the proposed hierarchical coordination, individual microgrids could supply backup power to each other, thus achieving a high-reliability and economical operation. The proposed coordination strategy for an islanded community microgrid will be discussed in Section V and verified by Case 2 in Section VI.

C. Hybrid Mode

Since each microgrid in Fig. 3 has their respective connection to the utility grid, the possibility exists that some microgrids are grid-connected while others are islanded. That is, the community microgrid is operating in hybrid mode, in which grid-connected and islanded microgrids operate as described in Section IV-A and IV-B, respectively. Here the islanded microgrids are still able to exchange power with other microgrids via the ac main bus, according to the set-points from CMC.

TABLE II
COMPARISON OF DROOP CONTROL IN MICROGRIDS AND THE PROPOSED HIERARCHICAL COORDINATION OF COMMUNITY MICROGRID

		Microgrid droop control	Proposed hierarchical coordination of a community microgrid
Functional component		Grid-forming DERs	IC_j (j=1,2,…N)
Variables	Monitored variables	f/V in the microgrid	f/V in MG_j and on the AC main bus (Normalization required)
	Controlled variables	Power output of a DER	Power export/import of MG_j
Control / Coordination	Primary (decentralized)	- Load sharing among DERs	- Initiate power import/export for MG_j in case of a deficient/surplus generation in MG_j
		- Real-time control of f/V	- Responds to f/V deviation that continuously exceeds a threshold
	Secondary (decentralized)	- Restore f/V without changing DER outputs	- Restore f/V in MG_j with small change on the exchanging power
		- Central or local detection (f/V), and local implementation	- Detect and implement at IC_j
	Tertiary (centralized)	Set-points for economic dispatch of DERs	Set-points for power exchange of each individual microgrid

V. COORDINATION IN ISLANDED COMMUNITY MICROGRID

The proposed community microgrid (Fig. 3) and the proposed hierarchical coordination strategy would provide significant reliability and economic benefits to individual microgrids especially when they are operating in island mode. Therefore, in this section, we will focus on the coordination strategy for an islanded community microgrid.

In island mode, microgrids with adequate generation capacity will serve their individual loads. They will also exchange power with other microgrids in the community when the operating point entering the shaded zone in Fig. 2. To highlight its novelty, the proposed hierarchical coordination strategy is compared with the existing microgrid droop control in Table II. As shown in this table, the proposed coordination strategy controls the power export/import of MG_j based on real-time monitoring f/V at IC_j; thus a decentralized, autonomous, and efficient coordination could be achieved without communication links between any two microgrids or high-bandwidth communications as discussed in Section III.

The proposed strategy includes the primary, secondary, and tertiary coordination. The primary and secondary are decentralized functions which are implemented at IC_j while the tertiary is a centralized management function, which are discussed in the rest of this section. The discussions in this section consider real power exchanges and the same analyses would equally correspond to reactive power exchanges.

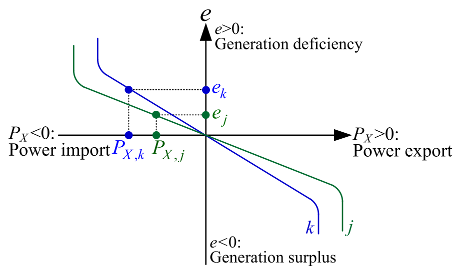

Fig. 4. Coordination droop characteristics in a community microgrid.

A. Primary Coordination in Island Mode

The primary coordination initiates the power export/import of MG_j by locally real-time detecting the f/V variations of ac main bus and that of MG_j. As summarized in Table II, the primary coordination only responds to f/V deviations that continuously exceed a threshold, which is highly desirable since it is unnecessary and uneconomical to initiate power exchanges in case of temporary f/V deviations (e.g., due to load change within MG_j).

A normalization process [14] is considered initially for bringing individual microgrid f/V to a common per-unit range. Equation (3) represents the normalization method in which the per-unit values of $f_j^{\text{p.u.}}$ and $V_{\mathrm{DC},j}^{\text{p.u.}}$ are 0, 1 or -1 when the original values are the rated, upper, or lower values, respectively. Upon normalization, the per-unit f/V of different microgrids are compared using (4). The positive/negative value of e_j that signals the generation deficiency/surplus in MG_j is then projected on the coordination droop curves in [14, Fig. 4]

$$f_j^{\text{p.u.}} = \begin{cases} \left(f_j - f_j^{\text{rated}}\right) \Big/ \left(f_j^{\max} - f_j^{\text{rated}}\right), \left(f_j > f_j^{\text{rated}}\right) \\ \left(f_j - f_j^{\text{rated}}\right) \Big/ \left(f_j^{\text{rated}} - f_j^{\min}\right), \left(f_j < f_j^{\text{rated}}\right) \end{cases}$$

$$V_{\mathrm{DC},j}^{\text{p.u.}} = \begin{cases} \dfrac{V_{\mathrm{DC},j} - V_{\mathrm{DC},j}^{\text{rated}}}{V_{\mathrm{DC},j}^{\max} - V_{\mathrm{DC},j}^{\text{rated}}}, \left(V_{\mathrm{DC},j} > V_{\mathrm{DC},j}^{\text{rated}}\right) \\ \dfrac{V_{\mathrm{DC},j} - V_{\mathrm{DC},j}^{\text{rated}}}{V_{\mathrm{DC},j}^{\text{rated}} - V_{\mathrm{DC},j}^{\min}}, \left(V_{\mathrm{DC},j} < V_{\mathrm{DC},j}^{\text{rated}}\right) \end{cases} \tag{3}$$

$$e_j = \begin{cases} f_0^{\text{p.u.}} - f_j^{\text{p.u.}} \quad (\text{for AC microgrid } \mathrm{MG}_j) \\ f_0^{\text{p.u.}} - V_{\mathrm{DC},j}^{\text{p.u.}} \quad (\text{for DC microgrid } \mathrm{MG}_j) \end{cases} \tag{4}$$
$$(j = 1, 2, \ldots, \mathrm{N}).$$

In Fig. 4, the coordination droop curves j and k are implemented at IC_j and IC_k to determine the power exchanges for MG_j and MG_k, respectively. For the proposed primary coordination, MG_0 acts as a slack bus for the community microgrid system, such that MG_j initially exchanges power with MG_0 (i.e., the ac main bus) based on IC_j coordination droop characteristics. That is, from MG_js point of view the rest of community is equivalent to one virtual DER, while MG_0 views each MG_j as a possible generation or load, as illustrated in Fig. 5(a) and (b), respectively. Thus a simplified and efficient coordination strategy could be achieved.

Fig. 6 illustrates the primary coordination in which the arrows represent the directions of power exchange flows.

1) In case of a power shortage, the f/V in MG_j would deviate as depicted by the shaded region in Fig. 2, causing a nonzero e_j according to (4).

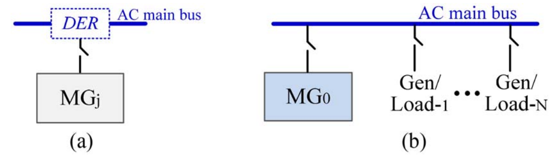

Fig. 5. Community microgrid from the perspective of (a) MG_j and (b) MG_0.

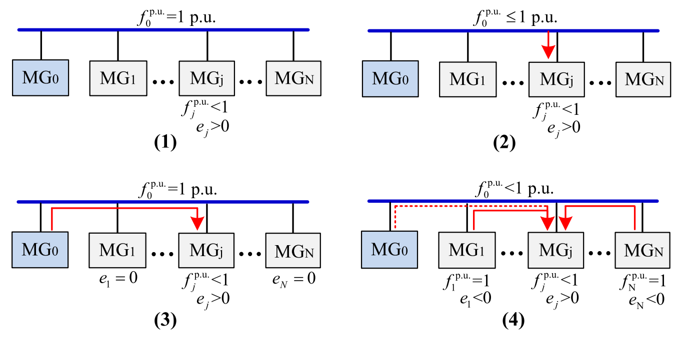

Fig. 6. Primary coordination. Primary coordination: 1) power shortage in MG_j; 2) power import to MG_j; 3) MG_0 supports the exchange; and 4) other microgrids support the exchange.

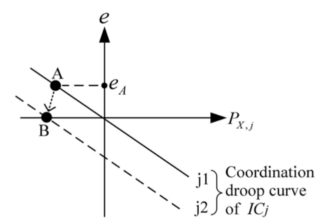

Fig. 7. Secondary coordination at IC_j.

2) The nonzero e_j would trigger IC_j to exchange power with the ac main bus, according to the coordination droop of IC_j as shown in Fig. 4.
3) With adequate generation capacity, MG_0 operating as a slack bus would adjust its DER dispatch for restoring the f/V to its rated value on the ac main bus.
4) If MG_0 does not have an adequate generation capacity for exchange, the f/V deviation on the ac main bus would result in nonzero values of e at other converter-coupled microgrids (i.e., $\mathrm{MG}_k, k = 1, 2, \ldots, N, k \neq j$). Accordingly, each MG_k would adjust its DER dispatch to serve the power exchange with MG_j, in which case the power flows are determined by the coordination droop characteristics at each IC_k as shown in Fig. 4.

B. Secondary Coordination in Island Mode

The secondary coordination concerns the f/V deviations as expressed by (5), where a nonzero power exchange ($P_{X,j}$) at steady state would require nonzero e_j at MG_j and thus impose an incremental error between $f_0^{\text{p.u.}}$ and $f_j^{\text{p.u.}}$ (assuming MG_j is an ac microgrid). Hence, f/V will be deviated from its rated value in MG_j which participates in power exchanges.

The secondary coordination at IC_j will shift the droop curves vertically so that microgrids can exchange power without compromising f/V. An example is provided in Fig. 7 which shows the coordination droop of IC_j. In this figure, originally MG_j exchanges power with the ac main bus

This article has been accepted for inclusion in a future issue of this journal. Content is final as presented, with the exception of pagination.

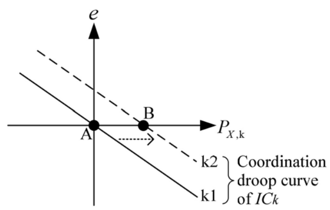

Fig. 8. Example of tertiary coordination.

at point-A (i.e., with a per-unit error of e_A). After shifting the droop curve from j_1 to j_2, the operating point will move to B, where the f/V of MG_j is restored to its rated values. Here, Fig. 7 shows a distinct difference between the proposed secondary coordination strategy and the existing secondary droop control as summarized in Table II. In Fig. 7, the value of $P_{X,j}$ at point-B is slightly larger than that at point-A, which is because when restoring the f/V of MG_j, the DER operating point in MG_j is shifted back from point-C to B in Fig. 2, where MG_j would require a slight higher power import

$$\begin{aligned} P_{\text{gen},j} + P_{X,j} &= P_{\text{load},j} \\ P_{X,j} = m_j \cdot e_j &= m_j \cdot \left(f_j^{\text{p.u.}} - f_0^{\text{p.u.}} \right). \end{aligned} \tag{5}$$

C. Tertiary Coordination in Island Mode

The proposed tertiary coordination ensures the optimal coordination of an islanded community microgrid by adjusting the power exchanges among microgrids. Note that tertiary coordination does not necessarily rely on the secondary coordination, which will be demonstrated by Scenario 2.3 in Section VI. The tertiary coordination is implemented using the centralized CMC computation and individual low-bandwidth communications with MCs as shown in Fig. 3. The following sequence of steps is followed for the tertiary coordination.

1) CMC obtains from each MC the microgrid information, including its reserve capacity, load condition, generation cost, power quality, etc.
2) At each time interval, CMC computes the optimal power exchange arrangement generally for economic purposes. The exchange could also consider factors other than economics. For example, as compared with MG_0, MG_k could deliver a higher quality of power; likewise, CMC could curtail load at MG_k and shift its generation to MG_j since MG_k has curtailable or shiftable load.
3) Using the optimal solution, CMC would adjust the set points for the coordination droops of ICs. For example, MG_j originally exchanges power with MG_0. However, CMC determined that it is more economical for MG_j to exchange power with MG_k; CMC then horizontally shifted the MG_ks coordination droop curve from k_1 to k_2 as shown in Fig. 8, where MG_k would exchange power with the ac main bus at point-B. Once stabilized, MG_k would replace MG_0 for the power exchange with MG_j.

D. IC Control Diagram

Fig. 9 shows the IC control diagram in which the computed reference $P_{X,j}^*$ is used to control IC_j power exchanges. In Fig. 9(a), $P_{X,j}^{\text{ref}}$ is optimized by the CMC which provides

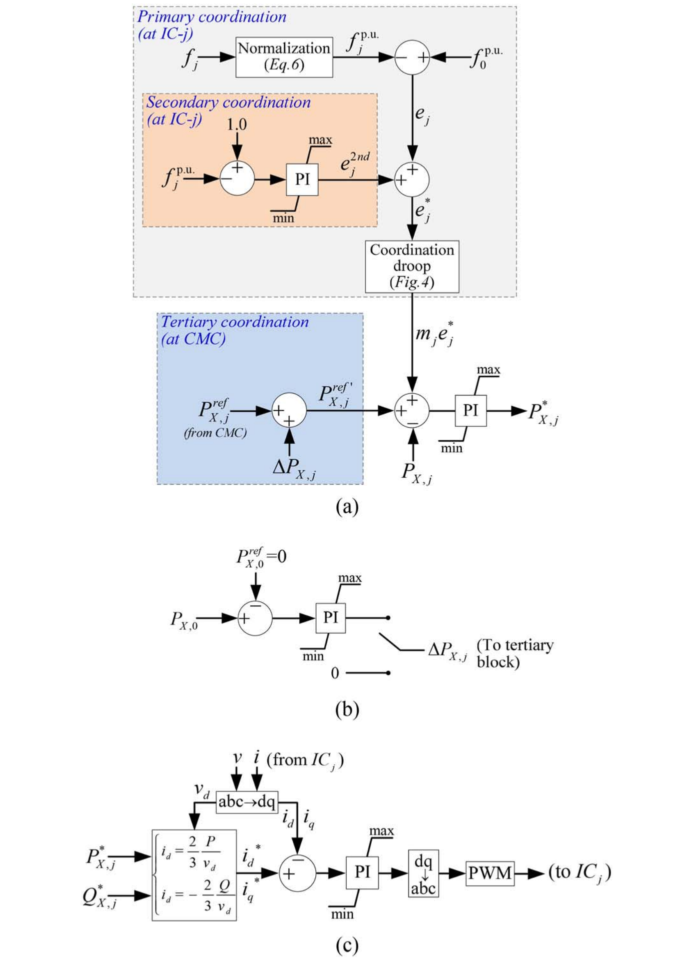

Fig. 9. Control diagrams of (a) hierarchical coordination, (b) adjustment signal in tertiary coordination, and (c) converter control.

the set point for power exchange. Additionally, an adjustment signal $\Delta P_{X,j}$ generated in Fig. 9(b) could be added onto the tertiary block to eliminate any steady state error in the tertiary coordination. Here, Fig. 9(b) provides an example of reducing MG_0 power exchange to zero. Based on Fig. 9(a), $P_{X,j}$ in the steady state can be expressed by (6) where it is assumed that IC_j adopts a linear coordination droop parameter m_j

$$P_{X,j} = P_{X,j}^{\text{ref}'} + m_j \left(e_j + e_j^{\text{2nd}} \right). \tag{6}$$

A similar hierarchical coordination strategy can be applied to the reactive power exchange. Therefore, the calculated reference for reactive power exchange ($Q_{X,j}^*$) is also added as an input to the converter control in Fig. 9(c).

VI. Numerical Simulation of Community Microgrid

This section presents the simulation cases for the operations of a community microgrid as shown in Fig. 10(a), in which the thick line represents the ac main bus and utility feeder and individual microgrids would be switched to islands once breaker B opens. This is a simplified version of Fig. 3 as grid-connected and island modes of a community microgrid are simulated in this section. The proposed strategy can be

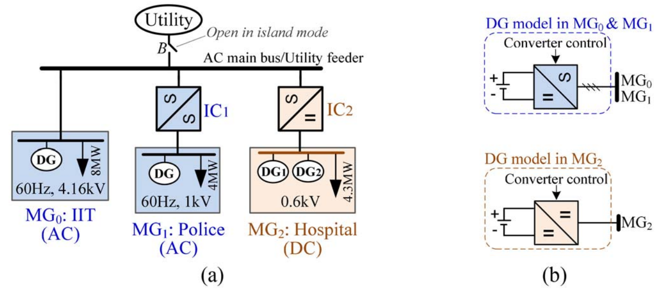

Fig. 10. Simulation setups. (a) Studied community microgrid. (b) DG models.

readily applied to the hybrid mode (see Section IV-C) which will be simulated in our future work. The community microgrid in Fig. 10(a) includes the IIT (a directly-connected ac microgrid denoted as MG0), a police station (a converter-coupled ac microgrid denoted as MG1), and a hospital (a converter-coupled dc microgrid denoted as MG2). IC1 and IC2 are interlinking-converters at MG1 and MG2, respectively. Fig. 10(a) also shows the rated frequency and voltage, number of DGs, and the total MW load of each microgrid. All DG units are modeled as converter-coupled dispatchable grid-forming DERs, as shown in Fig. 10(b), where the converter control module would implement the droop control within individual microgrids.

A few clarifying points are provided here.

1) The dc bus in Fig. 10(b) could represent a dc-type source or the dc terminal of an ac-to-dc converter in an ac-type source.
2) The proposed coordination strategy and simulations in this paper are not necessarily limited to converter-coupled DGs and are equally applied to directly-coupled dispatchable DGs (e.g., gas-turbine synchronous generators) that employ the droop control approach.
3) While the simulation setup in Fig. 10 may show some simplification, it provides a reasonable and adequate modeling in this paper as we focus on the coordinated strategy for power exchange among multiple microgrids.

For a further explanation on 1) and 2) and a detailed information on the DG modeling and control, please refer to [9]–[11].

Due to the limited space, we only provide simulation cases on real power exchanges in this section, and stress the point that similar processes corresponding to reactive power compensations in individual microgrids would fulfill reactive power exchange requirements in a community microgrid.

In our simulation results (depicted in Figs. 11–15), $V_{\text{dc}}^{\text{MG2}}$ is the per-unit dc bus voltage of the Hospital (MG2). PMG0, PMG1, PMG2, and Pgrid are power exchange (MW) of microgrids and the utility grid, where positive/negative MW values represent export/import flows, respectively. $P_{\text{gen}}^{\text{MG2}}$ and $P_{\text{load}}^{\text{MG2}}$ are the total generation and the total load (MW) in the Hospital (MG2).

A. Case 1: Operation of Grid-Connected Community Microgrid

Case 1 simulates the community microgrid in grid-connected mode using the discussions provided in Section IV-A. As shown by the simulation results in Fig. 11, before $t = 1$ s there is no power exchange between the utility grid and microgrids, which is due to the set points provided by each MC. Started at $t = 1, 2,$ and 3 s, MG_0, MG_1, and MG_2, respectively draw 0.05 MW from the utility grid, which is because MC_0, MC_1, and MC_2 actively decrease the local generations by 0.05 MW in respective microgrids. The f/V of each microgrid is maintained by the utility. Since the three microgrids are respectively grid-connected, they will not exchange power between each other.

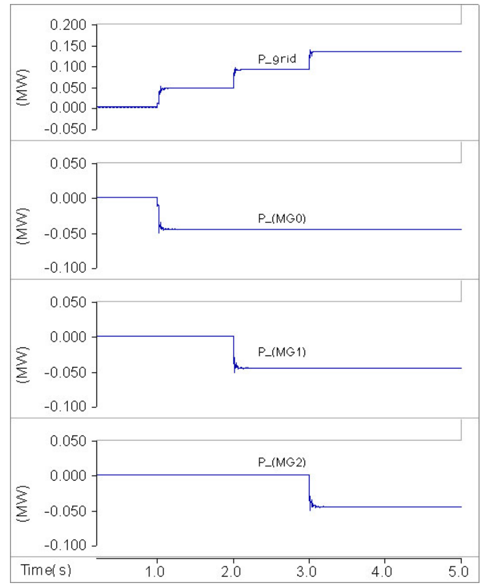

Fig. 11. Real power exchange flows in Case 1.

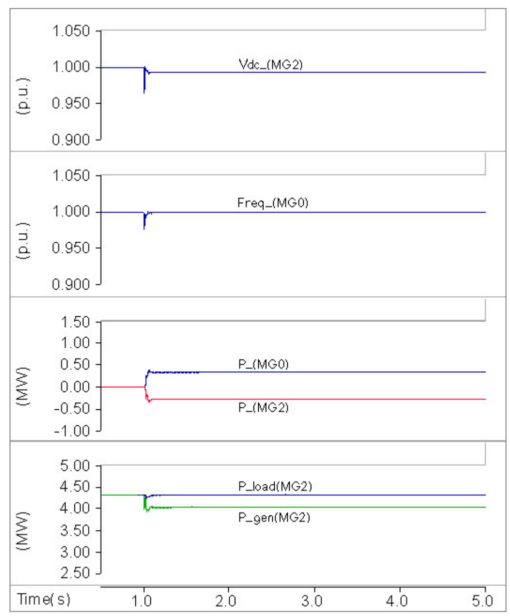

Fig. 12. Simulation results in Scenario 2.1 of Case 2.

B. Case 2: Coordination in Islanded Community Microgrid

In island mode, MG_0, MG_1, and MG_2 may exchange power based on the proposed hierarchical coordination strategy discussed in Section V. To verify the proposed strategy, four

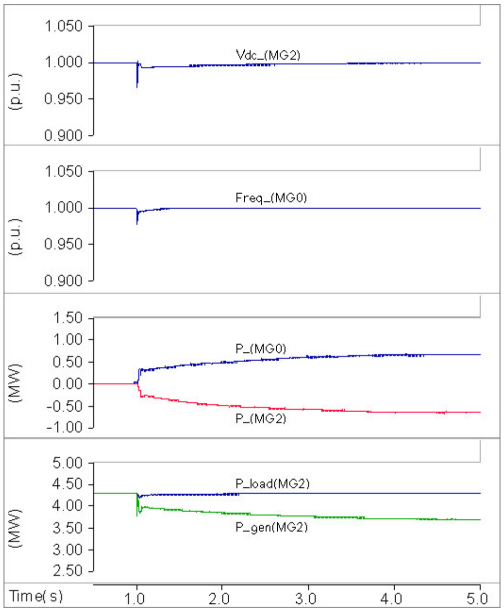

Fig. 13. Simulation results in Scenario 2.2 of Case 2.

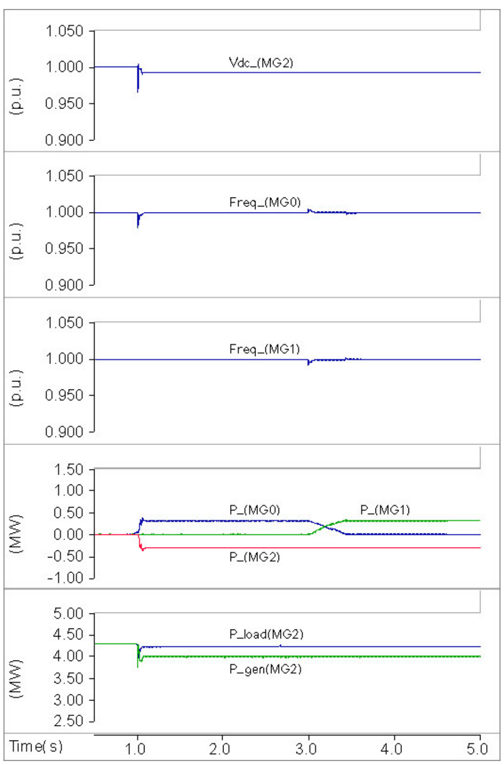

Fig. 14. Simulation results in Scenario 2.3 of Case 2.

scenarios will be simulated with the following settings for MG_2 parameters.

1) The total load in MG_2 is set at 4.3 MW.
2) In MG_2, P_B of DG_1 (see Fig. 2) is set at 3.7 MW.
3) DG_2 will be disconnected at $t = 1$ s (simulating a sudden loss of generation) to trigger the power import of MG_2.

In each scenario, the secondary or the tertiary coordination is either enabled or disabled as listed in Table III.

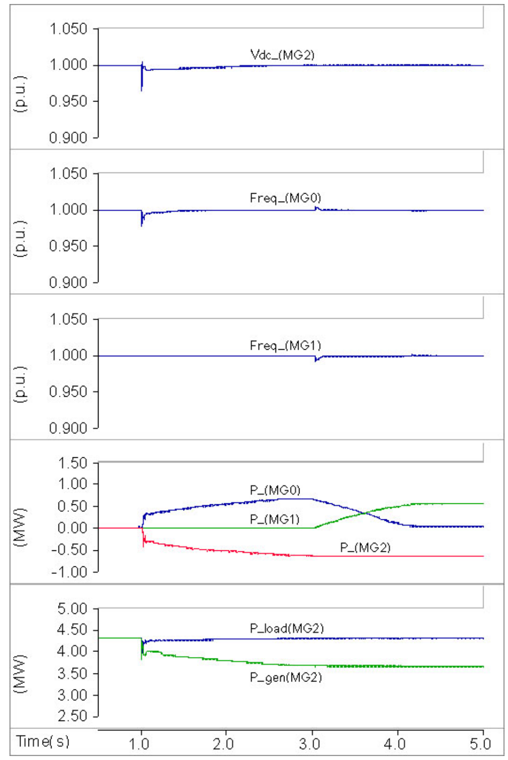

Fig. 15. Simulation results in Scenario 2.4 of Case 2.

TABLE III
COORDINATION STRATEGIES APPLIED IN THE FOUR SCENARIOS IN CASE 2

	Hierarchical coordination strategy		
	Primary	Secondary	Tertiary
Scenario 2.1	Enabled	----	----
Scenario 2.2	Enabled	Enabled	----
Scenario 2.3	Enabled	----	Starts at t=3s
Scenario 2.4	Enabled	Enabled	Starts at t=3s

1) Scenario 2.1: Primary Coordination: In this scenario, only the primary coordination is considered for power exchanges in island mode. As shown by the simulation results in Fig. 12, before $t = 1$ s, each microgrid serves its own load and there are no power exchanges. In MG_2, the 4.3 MW load is supplied by DG_1 (3.5 MW) and by DG_2 (0.8 MW). Since the 3.5 MW supplied by DG_1 is below its threshold of 3.7 MW, DG_1 is operating at point-A in Fig. 2. At $t = 1$ s, DG_2 in MG_2 is disconnected to simulate a generation outage. As indicated by P_{MG2} in Fig. 12, DG_1 increases its output briefly to 4.0 MW which is beyond its threshold, i.e., DG_1 moves from point-A to C in Fig. 2; therefore, V_{dc}^{MG2} drops to 0.99 p.u.

The V_{dc}^{MG2} drop initiates a 0.3 MW power flow from MG_0 to MG_2 based on the primary coordination, which is verified by (+0.3 MW) for P_{MG0} and (−0.3 MW) for P_{MG2} in Fig. 12. Note that here the values of V_{dc}^{MG2} (0.99 p.u.), DG_1 (4.0 MW), and power exchange (0.3 MW) represent the collaboration between the MG_2 droop (see Fig. 2) and the coordination droop (see Fig. 4).

V_{dc}^{MG2} will remain fixed at 0.99 p.u. after it drops from 1.0 p.u., which is because the secondary coordination is not applied. Here, the difference (0.01 p.u.) is used to maintain a fixed power exchange of 0.3 MW. In Fig. 12, MG_1 is not participating in any power exchange since the tertiary coordination is disabled in this scenario.

2) Scenario 2.2: Primary and Secondary Coordination: This scenario is the same as Scenario 2.1 except that the secondary coordination is enabled to verify the f/V capability of the proposed coordination strategy.

In Fig. 13, in a short period after $t = 1$ s, V_{dc}^{MG2} drops to 0.99 p.u., and the imported power and the local generation of MG_2 are changed rapidly to 0.3 and 4.0 MW, respectively, which are the same as those in Scenario 2.1. But in this scenario, V_{dc}^{MG2} is finally restored to 1 p.u., and the imported power and the local generation of MG_2 would increase to 0.6 MW and decrease to 3.7 MW, respectively. The different results obtained in this scenario can be explained as follows. First, at the community microgrid level, the secondary coordination vertically shifts the IC_2 curve (see Fig. 7) such that MG_2 can import power while maintaining V_{dc}^{MG2} at 1 p.u. Second, since V_{dc}^{MG2} is restored to 1 p.u., the operating point of DG_1 is then shifted back from point-C to B (see Fig. 2), which causes DG_1 to reduce its output from 4.0 to 3.7 MW (being equal to its threshold) and thus increases the imported power of MG_2 from 0.3 to 0.6 MW.

As verified in this scenario, the secondary coordination is able to maintain the rated f/V for individual microgrids that participate in the power exchange. Same as that in Scenario 2.1, the entire power exchange in this scenario is provided by MG_0 which is due to the absence of tertiary coordination.

3) Scenario 2.3: Primary and Tertiary Coordination: This scenario is the same as Scenario 2.1 except that tertiary coordination is started at $t = 3$ s to prove the ability of the tertiary coordination in adjusting the power exchange. Here it is assumed that MG_2 has a lower marginal cost than that in MG_0. The secondary coordination is disabled in this scenario in order to demonstrate that the tertiary coordination does not necessarily depend on the secondary coordination.

In Fig. 14, during 1–3 s, the imported power of MG_2 is provided by MG_0, which is the same as that in Scenarios 2.1 and 2.2. At $t = 3$ s, since the tertiary coordination is started by CMC, the power export of MG_0 is reduced to zero and MG_1 begins to export 0.3 MW, i.e., MG_1 replaces MG_0 to deliver power to MG_2. This outcome can be explained using Fig. 8: at $t = 3$ s the tertiary coordination shifts the curve of IC_1 to the right thus increases its power export set-point to 0.3 MW, which is the value of $P_{X,j}^{ref'}$ in Fig. 9(a) [computed by Fig. 9(b)]. Accordingly, MG_1 would export 0.3 MW to the ac main bus and the power export of MG_0 is reduced to zero.

As shown in Fig. 14, V_{dc}^{MG2} will remain fixed at 0.99 p.u. after it is lowered. This is because the secondary coordination is not applied, which is the same as that in Scenario 2.1. This scenario verifies the role of tertiary coordination and demonstrates that the tertiary coordination can be implemented independent of the secondary coordination.

4) Scenario 2.4: Hierarchical Coordination: Primary, secondary, and tertiary coordination are applied in this scenario for verifying the hierarchical coordination strategy proposed in this paper. Fig. 15 shows that the simulation results incorporate the features presented in Scenarios 2.2 and 2.3.

In this figure, V_{dc}^{MG2} is lowered to 0.99 p.u. and then restored to 1 p.u., the imported power and the local generation of MG_2 are rapidly changed to 0.3 and 4.0 MW, respectively, and then the two values are increased to 0.6 MW and decreased to 3.7 MW, respectively, as we applied the secondary coordination which is the same as that in Scenario 2.2.

On the other hand, from $t = 3$ s, MG_1 starts to export power and finally replaces MG_0 for delivering power to MG_2, as we applied the tertiary coordination the same way as that in Scenario 2.3. The simulation results in this scenario successfully verify the functions of primary, secondary, and tertiary coordination in the proposed hierarchical coordination strategy. While the real power coordination is simulated in this section, the same strategy would apply to the reactive power coordination.

VII. Conclusion

This paper proposed a hierarchical coordination strategy for ensuring the optimal power exchanges among microgrids in an islanded community microgrid. The proposed coordination strategy also applies to the grid-connected operation of community microgrid. In the proposed strategy, the primary and secondary coordination are decentralized functions executed by the interlinking-converter of individual microgrids. The primary coordination initiates the power exchanges based on locally monitoring the frequency and voltage deviations while the secondary coordination maintaining the frequencies and voltages at rated values for each microgrid. The tertiary coordination, which is a centralized management function at the community level, ensures the optimal and economic operation of the community microgrid by adjusting the power exchange flows.

The proposed hierarchical coordination strategy is applied to a community microgrid model which included three ac and dc microgrids. The simulation cases address the islanded and grid-connected operations of community microgrid. The simulation results have successfully proven that the proposed coordination strategy is able to initiate the power exchanges when one or more microgrids encounters power shortage, while maintaining the rated frequency and voltage for each participating microgrid and economically optimizing the exchanged power, thus ensuring an economic, efficient, and flexible coordination of a community microgrid.

Acknowledgment

The authors would like to thank the technical support provided by the Science and Technology Unit, King Abdulaziz University, Jeddah, Saudi Arabia.

REFERENCES

[1] R. H. Lasseter, "Microgrids," in *Proc. 2002 IEEE Power Eng. Soc. Winter Meeting*, New York, NY, USA, 2002, pp. 305–308.

[2] F. Katiraei, R. Iravani, N. Hatziargyriou, and A. Dimeas, "Microgrids management," *IEEE Power Energy Mag.*, vol. 6, no. 3, pp. 54–65, May/Jun. 2008.

[3] J. C. Vasquez, J. M. Guerrero, J. Miret, M. Castilla, and L. G. de Vicuña, "Hierarchical control of intelligent microgrids," *IEEE Ind. Electron. Mag.*, vol. 4, no. 4, pp. 23–29, Dec. 2010.

[4] J. M. Guerrero, J. C. Vasquez, J. Matas, L. G. de Vicuña, and M. Castilla, "Hierarchical control of droop-controlled AC and DC microgrids—A general approach toward standardization," *IEEE Trans. Ind. Electron.*, vol. 58, no. 1, pp. 158–172, Jan. 2011.

[5] J. M. Guerrero, M. Chandorkar, T. Lee, and P. C. Loh, "Advanced control architectures for intelligent microgrids—Part I: Decentralized and hierarchical control," *IEEE Trans. Ind. Electron.*, vol. 60, no. 4, pp. 1254–1262, Apr. 2013.

[6] (2012). *Microgrid Project at IIT*. [Online]. Available: http://www.iitmicrogrid.net/microgrid.aspx

[7] B. T. Patterson, "DC, come home: DC microgrids and the birth of the 'Enernet,'" *IEEE Power Energy Mag.*, vol. 10, no. 6, pp. 60–69, Nov./Dec. 2012.

[8] L. Che, M. E. Khodayar, and M. Shahidehpour, "Adaptive protection system for microgrids: Protection practices of a functional microgrid system," *IEEE Electrif. Mag.*, vol. 2, no. 1, pp. 66–80, Mar. 2014.

[9] M. Shahidehpour and M. E. Khodayar, "Cutting campus energy costs with hierarchical control: The economical and reliable operation of a microgrid," *IEEE Electrif. Mag.*, vol. 1, no. 1, pp. 40–56, Sep. 2013.

[10] L. Che, M. Khodayar, and M. Shahidehpour, "Only connect: Microgrids for distribution system restoration," *IEEE Power Energy Mag.*, vol. 12, no. 1, pp. 70–81, Jan./Feb. 2014.

[11] L. Che and M. Shahidehpour, "DC microgrids: Economic operation and enhancement of resilience by hierarchical control," *IEEE Trans. Smart Grid*, vol. 5, no. 5, pp. 2517–2526, Sep. 2014.

[12] T. Dragicevic, J. M. Guerrero, J. C. Vasquez, and D. Skrlec, "Supervisory control of adaptive-droop regulated DC microgrid with battery," *IEEE Trans. Power Electron.*, vol. 29, no. 2, pp. 695–706, Feb. 2014.

[13] X. Liu, P. Wang, and P. C. Loh, "A hybrid AC/DC microgrid and its coordination control," *IEEE Trans. Smart Grid*, vol. 2, no. 2, pp. 278–286, Jun. 2011.

[14] P. C. Loh, L. Ding. Y. Chai, and F. Blaabjerg, "Autonomous operation of hybrid microgrid with AC and DC subgrids," *IEEE Trans. Power Electron*., vol. 28, no. 5, pp. 2214–2223, May 2013.

[15] R. Majumder, "A hybrid microgrid with DC connection at back to back converters," *IEEE Trans. Smart Grid*, vol. 5, no. 1, pp. 251–259, Jan. 2014.

[16] N. Eghtedarpour and E. Farjah, "Power control and management in a hybrid AC/DC microgrid," *IEEE Trans. Smart Grid*, vol. 5, no. 3, pp. 1–12, Apr. 2014.

[17] P. Wang *et.al*., "Distributed control for autonomous operation of a three-port AC/DC/DS hybrid microgrid," *IEEE Trans. Power Electron.*, vol. 62, no. 2, pp. 1279–1290, Feb. 2015.

[18] E. J. Ng and R. A. El-Shatshat, "Multi-microgrid control systems (MMCS)," in *Proc. IEEE Power Energy Soc. Gen. Meeting*, Minneapolis, MN, USA, Jul. 2010, pp. 1–6.

[19] L. Mariam, M. Basu, and M. F. Conlon, "Community microgrid based on micro-wind generation system," in *Proc. 48th Int. Univ. Power Eng. Conf. (UPEC),* Dublin, Ireland, Sep. 2013, pp. 1–6.

[20] L. Mariam, M. Basu, and M. F. Conlon, "Development of a simulation model for a community microgrid system," in *Proc. 49th Int. Univ. Power Eng. Conf. (UPEC),* Cluj-Napoca, Romania, Sep. 2014, pp. 1–6.

Liang Che (S'14) received the B.S. degree from Shanghai Jiaotong University, Shanghai, China, in 2006, and the M.S. degree from the Illinois Institute of Technology, Chicago, IL, USA, in 2013, where he is currently pursuing the Ph.D. degree, all in electrical engineering.

His current research interests include microgrid operation, planning, and optimization.

Mohammad Shahidehpour (F'01) received the Honorary Doctorate degree from the Polytechnic University of Bucharest, Bucharest, Romania, in 2009.

He is the Bodine Chair Professor and a Director of the R. W. Galvin Center for Electricity Innovation, Illinois Institute of Technology, Chicago, IL, USA, and a Research Professor with King Abdulaziz University, Jeddah, Saudi Arabia.

Ahmed Alabdulwahab received the Ph.D. degree in electrical engineering from the University of Saskatchewan, Saskatoon, SK, Canada, in 2003.

He was a Consultant at the Electricity and Co-Generation Regulatory Authority, Saudi Arabia, and a Visiting Scientist at Kinectrics, Inc., Toronto, ON, Canada, and the University of Manchester, Manchester, U.K. He is an Associate Professor with the Department of Electrical Engineering and Computer Engineering, and is affiliated with the Renewable Energy Research Group, King Abdulaziz University, Jeddah, Saudi Arabia. His current research interests include power system planning and reliability evaluations.

Yusuf Al-Turki received the Ph.D. degree in power systems from the University of Manchester, Manchester, U.K., in 1985.

Since 1999, he has been a Professor with the Department of Electrical and Computer Engineering, King Abdulaziz University, Jeddah, Saudi Arabia, where he is currently the Dean of Research. His current research interests include system modeling, power system dynamics, renewable energy, and microgrids.